How Polyelectrolyte Adsorption Depends on History: A Combined Fourier Transform Infrared Spectroscopy in Attenuated Total Reflection and Surface Forces Study

Svetlana A. Sukhishvili, Ali Dhinojwala,† and Steve Granick*

Department of Materials Science and Engineering, University of Illinois, Urbana, Illinois 61801

Received June 1, 1999. In Final Form: August 11, 1999

We present a systematic study of how adsorption history affects the thickness, surface forces, and interfacial rheology of a model cationic polymer. The polymer was quaternized poly-4-vinylpyridine, QPVP (weight-average degree of polymerization $n_w = 325$ and 98% quaternized with ethyl bromide). The main comparisons concerned one-step adsorption from solution at a variable salt concentration up to 0.5 M NaCl, versus two-step adsorption (initial adsorption from buffer solution without added salt, then NaCl added later). The aqueous solutions were buffered at pH = 9.2 such that the surfaces (mica in the case of surfaces forces (SFA) experiments, oxidized silicon in the case of in situ infrared (FTIR-ATR) experiments) in each case carried a large negative charge. The SFA and FTIR-ATR experiments gave consistent estimates of the amount of polymer adsorbed, confirming the expectation that adsorption should be driven by electrostatic attraction to the surface of large opposite charge. The adsorbed amount showed little dependence on path, validating the common assumption of equilibration in this respect. However the layer thickness measured by surface forces, the shear nanorheology response at a given surface force, and the dichroism of pendant side groups of the polymer all showed a pronounced dependence on the path to reach the adsorbed state. We interpret the measurements to suggest that two-step adsorption produces an inhomogeneous layer comprised of a dense layer of segments closest to the solid surface and a sparse outer layer. In particular, two-step adsorption produced thicker layers and a greater tendency to decouple shear forces from those that resist compression in the normal direction, thereby lessening the shear forces at a given level of normal force.

Introduction

Adsorption of charged polymers is prone, because Coulombic sticking to a surface is not weak, to show dependence on history. These problems of charged polymers, commonly called "polyelectrolytes", combine some of the most fundamental problems of polymer physics and of electrolyte interactions in aqueous solution. We are interested here in understanding polyelectrolytes adsorbed from solution to solid surfaces. The problem has seen burgeoning interest recently, with much theoretical as well as experimental activity, but progress has been limited by the paucity of experimental techniques capable of probing directly the features of these adsorbed layers. The experimental difficulty is that the adsorbed amount is very small (typically on the order of just 1 mg m^{-2}, i.e., 0.1 μg cm^{-2}) and the adsorbed layer is buried between macroscopic phases (the adsorbing solid and the bulk liquid solution); it is difficult to find direct experimental probes capable of distinguishing the problem at hand from overwhelming influences of the two surrounding bulk phases. The main point of the study presented below is to present experimental observations derived from the conjunction of two independent quantitative instrumental methods which share the feature that both static and dynamic features of adsorbed polyelectrolyte layers were probed in situ. Our experimental findings suggest that the dependence of adsorbed layer structure on the *history* or *path dependence* of adsorption can be understood in systematic terms.

When one considers past work on this problem, much attention has been given to the theoretical prediction of configurations of charged polymer chains bound to a surface by electrostatic interactions. The supposition is, nearly always, statistical mechanical equilibration.[1−8] Experiments, conversely, have accumulated much evidence that polyelectrolyte chains may adsorb with configurations that depend on the details of the adsorption process. Sufficiently long equilibration would of course, in principle, erase all history dependence, but experiments show that the time required can be longer than reasonable experimental time scales. There are at least two pieces of evidence for this proposition. One piece of evidence is endemic heterogeneity, recently found even for adsorption onto surfaces for which there was good reason to suppose homogeneity of the surface chemistry.[9−11] This is consistent with the proposition that structural equilibration is very slow between those chains that first arrive at the initially bare solid surface and become consequently highly flattened and later-arriving chains are forced to adopt more fluffy conformations because many of the potential adsorption sites were already occupied. The result is conformational inhomogeneity over experimentally rel-

† Current address: Department of Polymer Science, University of Akron, Akron, Ohio 44325.

(1) Hesselink, F. Th. *J. Colloid Interface Sci.* **1977**, *60*, 448.
(2) Muthukumar, M. *J. Chem. Phys.* **1987**, *86*, 7230.
(3) Borisov, O. V.; Zhulina, E. B.; Birshtein, T. M. *J. Phys. II* **1994**, *4*, 913.
(4) Shubin, V.; Linse, P. *J. Phys. Chem.* **1995**, *99*, 1285.
(5) Böhmer, M. R.; Evers, O. A.; Scheutjens, J. M. H. M. *Macromolecules* **1990**, *23*, 2288.
(6) van de Steeg, H. G. M.; Cohen Stuart, M. A.; de Keizer, A.; Bijsterbosch, B. H. *Langmuir* **1992**, *8*, 2538.
(7) Linse, P. *Macromolecules* **1996**, *29*, 326.
(8) Châtellier, X.; Joanny, J. F. *Phys. Rev. E* **1998**, *57* (6), 6923.
(9) Tanaka, H.; Swerin, A.; Ödberg, L. *Langmuir* **1994**, *10*, 3466.
(10) Hoogeveen, N. G.; Cohen Stuart, M. A.; Fleer, G. J. *J. Colloid Interface Sci.* **1996**, *182*, 146.
(11) Sukhishvili, S. A.; Granick, S. *J. Chem. Phys.* **1998**, *109*, 6869.

10.1021/la990679o CCC: $18.00
Published on Web 09/29/1999

evant time scales, but in most cases the evidence in support of this proposition was indirect and qualitative.

A second piece of evidence comes from experiments designed to quantitatively measure the actual equilibration time. The common route has been to compare adsorbed layers with different formation history. Usually the polyelectrolyte was allowed to adsorb under some given condition, then this condition (the salt concentration or the supply rate of polymer solution to the surface) was changed.[12−15] Apart from a few experiments in which very fast reorganization rates were inferred,[14] studies of this kind have found adsorbed polyelectrolyte layers to exhibit very slow equilibration to altered ambient conditions—typically, longer than was experimentally achievable. A related finding is that adsorption was strongly hysteretic. Many results of this kind were summarized in a recent review.[16] Nonequilibrated structure was also suggested by recent measurements of the normal forces acting between two surfaces bearing bound polyelectrolyte.[15,17] Recently it was suggested that origins of this endemically slow structural relaxation can be found in part in the strong electrostatic sticking energy of charged polyelectrolyte segments to a surface in an ionic environment (this was deduced to be in the range $4-7\ k_BT$ for different polymers and various concentrations of inorganic salts) and in part in the higher stiffness of polyelectrolyte chains compared to uncharged polymers.[18,19] The dependence of nonequilibrated polymer conformations on salt concentration was not directly addressed in these prior studies, however.

Seeking to reconcile the inconsistency between the equilibrium-based theories and the overwhelming experimental finding that features of the adsorbed layers depend on the way they were built, an attempt to introduce a nonequilibrium theory was made some years ago,[20] but it did not receive further development.

Let us consider the possibility of having the same adsorbed amount of polymer but different structure (different segmental density profiles). The polymer might in principle form a thin but dense layer or a thick but loose layer. In other words, changes of the segmental density in the direction normal to the surface might be abrupt or gradual. The former possibility, the abrupt change, was given the evocative name, "hairy carpet", by Varoqui and co-workers.[21] Deliberate manipulation between these two extremes might produce a variety of interesting surface structures possessing different chemical properties (in the case of functional polymers) and certainly different hydrodynamic and viscoelastic properties. Understanding these structures and their properties would represent a new and challenging scientific problem and might have technological ramifications in wide-ranging areas, from lubrication and processing of colloidal dispersions, to the engineering of biocompatibility and bioseparation processes. The following specific questions should be answered: (1) How to predict how the structure of these hysteretic layers depends on the formation history? (2) How to make use of this phenomenon of metastability to build polyelectrolyte layers whose segmental density in the direction normal to the surface is tailored intentionally?

Our emphasis in the present study was to study systematically how history-dependent structures could be manipulated by changing the ionic strength of inorganic salts in the ambient aqueous solution. To this end, we made use of two complementary experimental techniques. First, Fourier transform infrared spectroscopy in attenuated total reflection (FTIR-ATR) gave numbers concerning not only mass adsorbed but also average orientation of the absorbing species relative to the surface. Second, we used a dynamic surface forces apparatus (SFA) to measure dynamic as well as static forces. Because it was not practicable to perform these two independent experiments using the same solid surface, both studies were performed at high pH such that the solid surfaces (oxidized silicon for FTIR-ATR experiments, mica for SFA experiments) would carry so large a negative charge that adsorption of the polyelectrolyte would, in both cases, be driven in a similar way by electrostatic attraction to the surface although the surfaces were chemically different. The combination of these two techniques has provided us with joint information about segmental orientation, extension of the adsorbed layer normal to the surface, and viscoelastic properties.

Experimental Section

Materials. Poly-4-vinylpyridine (PVP) was selected for study because it is relatively easy to quaternize this polymer to near completion using well-established methods.[22,23] We refer below to quaternized PVP by the acronym, QPVP. The parent PVP sample with weight-average molecular weight $M_w = 34\ 200$ g mol^{-1} (weight-average degree of polymerization $n_w = 325$) and the ratio of weight-average to number-average molecular weight $M_w/M_n = 1.23$ was purchased from Polymer Source, Québec, Canada. This sample, synthesized by anionic polymerization, was characterized according to manufacturer's specifications by a degree of stereoregularity of 70%. Quaternization was carried out by us in 10 wt % ethanol solution containing PVP with 5-fold excess of ethyl bromide at 60 °C under inert N_2 atmosphere. The reaction was terminated after 12 h by precipitating the polymer into diethyl ether to obtain a polymer with 98% of quaternized pyridine repeat units (characterized by us by quantifying the ratio of quaternized to unreacted pyridine rings using infrared spectroscopy).

The inorganic salts (General Storage, pure grade, or Aldrich, purissium grade) were used as received after control experiments showed no difference if they were baked first at 600 °C to burn out conceivable organic contaminants.

The H_2O was double-distilled and then further purified by passage through Milli-Q (Millipore) deionizing and filtration columns. Deuterium oxide with 99.9% isotope content was obtained from Cambridge Isotope Laboratories and used without further purification. The results obtained using this solvent were always consistent with those obtained using purified H_2O, indicating that D_2O lacked impurities that interfered with the adsorption process. As a matter of terminology, when experiments were performed in D_2O rather than H_2O, we will refer to pD rather than pH.

Methods. FTIR-ATR Measurements. Infrared spectra were collected using a Biorad FTS-60 Fourier transform infrared spectrometer (FTIR) equipped with a broad-band mercury cadmium telluride detector. The attenuated total reflection (ATR) optics and the thermostated home-built adsorption cell placed

(12) Meadows, J.; Williams, P. A.; Garvey, M. J.; Harrop, R. A.; Phillips, G. O. *Colloids Surf.* **1988**, *32*, 275.
(13) Pefferkorn, E.; Jean-Chronberg, A. C.; Varoqui, R. *Macromolecules* **1990**, *23*, 1735.
(14) Ödberg, L.; Sandberg, S.; Welin-Klintström, S.; Arwin, H. *Langmuir* **1995**, *11*, 2621.
(15) Dahlgren, M. A. G.; Hollenberg, H. C. M.; Claesson, P. M. *Langmuir* **1995**, *11*, 4480.
(16) Vandeven, T. G. M. *Adv. Colloid Interface Sci.* **1994**, *48*, 121.
(17) Luckham, P. F.; Klein, J. *J. Chem. Soc., Faraday Trans. 1* **1984**, *80*, 865.
(18) Denoyel, R.; Durand, G.; Lafuma, F.; Audebert, R. *J. Colloid Interface Sci.* **1990**, *139*, 281.
(19) Sukhishvili, S. A.; Granick, S. *J. Chem. Phys.* **1998**, *109*, 6861.
(20) Barford, W.; Ball, R. C.; Nex, C. M. M. *J. Chem. Soc., Faraday Trans. 1* **1986**, *82*, 3233.
(21) Pefferkorn, E.; Haouam, A.; Varoqui, R. *Macromolecules* **1989**, *22*, 2677.
(22) Fuoss, R. M.; Strauss, U. P. *J. Polym. Sci.* **1948**, *3*, 246.
(23) Margolin, A. L.; Izumrudov, V. A.; Švedas, V. K.; Zezin, A. B.; Kabanov, V. A.; Berezin, I. V. *Biochim. Biophys. Acta* **1981**, *660*, 359.

in a nitrogen-purged compartment external to the FTIR spectrometer were described previously.[24] Spectra in orthogonal p and s polarizations were obtained by switching a wire-grid polarizer (Graesby/Specac).

The temperature, regulated by circulation of water through a jacket surrounding the metal enclosure of the ATR cell, was 25.0 °C. The ATR surface was a rectangular trapezoidal Si crystal of dimension 50 mm × 20 mm × 2 mm (Harrick Scientific) whose beam entrance and exit surfaces were cut at 45°. The methods to controllably oxidize the crystal surface and to clean the cell elements were described elsewhere.[25] These methods of surface preparation yielded adsorption measurements that were quantitatively reproducible from experiment to experiment.

Interferograms were collected in p and s polarization with 4 cm^{-1} resolution. To collect each interferogram, the number of averaged scans was 512. To obtain the spectra analyzed below, each absorbance spectrum was ratioed to a corresponding background, measured for the same ATR cell in the absence of polymer but with the same polarization of the incident beam, and the same D_2O buffer solution containing the same concentration of inorganic salts.

The infrared absorption peaks were integrated using curve-fitting of the absorption peaks obtained in p and s polarizations. The total infrared absorbance was the sum of these values, $A \equiv A_p + A_s$. The most consistent results were obtained when 90% of the peaks were assumed to be Gaussian and 10% to be Lorenzian. The peak centers and bandwidths were not fixed, but the results of the curve-fitting were carefully checked for consistency in these parameters. In curve-fitting, a baseline correction was performed to the raw spectra.

Owing to the large penetration depth of the evanescent wave relative to thickness of the adsorbed layer (for example, the penetration depth of the evanescent wave was 0.47 μm at 1643 cm^{-1} for the silicon crystal that we used), these measurements included contributions from oscillators in the isotropic polymer solution in addition to those within the adsorbed polymer layers. To separate their respective contributions, the polymer solution was sometimes replaced by the pure buffer in order to provide a direct calibration of the solution contribution. While doing so, the adsorbed polyelectrolyte molecules remained irreversibly bound to the surface of silicon crystal. In other experiments, this calibrated solution contribution was subtracted from the total absorbance to obtain that attributable solely to adsorbed polymer. The subtracted value was roughly 25% of the total signal for a solution concentration of 1 mg mL^{-1} and proportionately less for more dilute QPVP solutions described below.

The adsorbed amount was calibrated from the absorptivity of QPVP in bulk solution, measured independently, as summarized in more detail elsewhere.[19,24,25] In brief, QPVP solutions of known concentrations were brought into contact with a saturated adsorbed layer, so that this surface could be considered as essentially nonadsorbing as a substrate for additional adsorption. Analysis of the slope of the integrated absorbance of the 1643 cm^{-1} absorbance band as a function of the solution concentration of QPVP gave the extinction coefficient of 0.0066 absorbance units mg^{-1} mL^{-1}. From this number and the known value of penetration depth, the calibration constant to infer the adsorbed amount of QPVP was obtained; it was 0.028 absorbance units m^2 mg^{-1}.

We also found that absorbance of this band did not change as salt concentration was varied between 0.001 M in pure buffer to 0.5 M NaCl, thus showing that the molecular absorptivity of QPVP did not depend on the salt concentration.

Dichroism Measurements. To infer orientation information from the infrared spectra, we used the dichroic ratio, D, defined as the ratio of absorptivities for p and s polarizations, $D \equiv A_p/A_s$. For a model in which a transition moment of the vibration is only allowed to rotate freely within the XY plane while keeping constant angle ϕ with the surface normal[26,27]

$$D \equiv A_p/A_s = (E_x^2 + 2E_z^2 \operatorname{ctg}^2 \phi)/E_y^2 \quad (1)$$

where E_x and E_y are the amplitudes of the electric field at the interface lying in the plane of the crystal surface and E_z is perpendicular to it. These amplitudes can be easily derived from the known angle of incidence of the IR beam and the known refractive indices of the crystal (3.42 for silicon) and the solvent (1.32 for D_2O). These values were found to be $E_x = 1.39$, $E_y = 1.5348$, and $E_z = 1.66$. Here x and y are Cartesian directions in the plane of the surface and z is normal to it. For a random array of the molecules (or for the molecules aligned on the surface with a "magic angle" of 54.7° to the surface normal)

$$D = (E_x^2 + E_z^2)/E_y^2 \quad (2)$$

which yields 2.05 for our case. Values of $D < 2.05$ indicate alignment of the transition moment preferentially parallel to the surface ($D = 0.82$ for perfectly parallel alignment), and $D > 2.05$ indicates preferentially vertical orientation ($D \rightarrow \infty$ for a perfectly vertical array).

One complication, for the case when the refractive index of the thin layer of adsorbed molecules is different from that of the solvent, is that the E_z component of the electric field should be corrected by the ratio of the refractive indices of the solvent and the adsorbed layer. But this correction is minimal, as was shown before for the similar system.[28]

Measurements with the Dynamic Surface Force Apparatus. Force−distance profiles (static forces required to compress the films to a given thickness) and dynamic oscillatory shear forces were measured using the modified surface force apparatus that has been described in detail elsewhere.[29] The surfaces were comprised of thin freshly cleaved step-free sheets of muscovite mica glued onto cylindrically shaped silica lenses; the resulting cylindrical shapes of mica were positioned in orthogonal directions so that they would produce a point contact when brought close together. The bottom surface was stationary during a shear experiment, and the top surface was suspended as a boat from two piezoelectric bimorphs. As a sinusoidal shear force was applied to the system by applying sinusoidal voltage to one bimorph from which it was suspended (the "sender"), motion was resisted by viscoelastic properties of the fluid layer between the two surfaces. The damping and phase shift of oscillation were detected from the voltage induced in the symmetrically placed "receiver" piezoelectric bimorph from which it was also suspended. The damping and phase shift were used to calculate the complex shear force, within the fluid layer, that resisted motion.

The forces were represented as an elastic force, in phase with the drive, and a dissipative force, out of phase with the drive. In previous work we sometimes used estimates of the effective contact area between crossed cylinders to calculate an effective shear modulus.[30] In many of the graphs presented below we will avoid this assumption and simply normalize force by displacement. We obtain the force constants of the confined fluid after correcting for the calibrated apparatus compliance, to give two spring constants of the confined liquid (L): an elastic and a dissipative spring constant, k_L and ωb_L, respectively.

To introduce the sample into the apparatus, a few drops of QPVP solution were inserted between the opposed mica sheets using a clean glass pipet. As described previously, dynamic experiments in an aqueous environment were much more difficult than those run in dry hydrocarbon environments owing to drifts of the piezoelectric circuitry.[31] This limited the lifetime of any experiment to a few hours and precluded making measurements at variable frequencies in addition to variable film thicknesses. As described previously,[31] equilibrating the bimorphs in the humid environment for several hours before commencing the experiment improved their stability.

Results and Discussion

I. Adsorption as a Function of Ionic Strength. I.A. FTIR-ATR Measurements. Representative FTIR-

(24) Frantz, P.; Granick, S. *Macromolecules* **1995**, *28*, 6915.
(25) Frantz, P.; Granick, S. *Langmuir* **1992**, *8*, 1176.
(26) Frey, S.; Tamm, L. K. *Biophys. J.* **1991**, *60*, 922.
(27) Sperline, R. P.; Song, Y.; Y. Freiser, Y. *Langmuir* **1992**, *8*, 2183.
(28) Sukhishvili, S. A.; Granick, S. *J. Phys. Chem. B* **1999**, *103*, 472.
(29) Peachey, J.; Van Alsten, J.; Granick, S. *Rev. Sci. Instrum.* **1991**, *62*, 463.
(30) Peanasky, J.; Cai, L.; Granick, S.; Kessel, C. R. *Langmuir* **1994**, *10*, 3874.
(31) Dhinojwala, A.; Granick, S. *J. Am. Chem. Soc.* **1997**, *119*, 241.

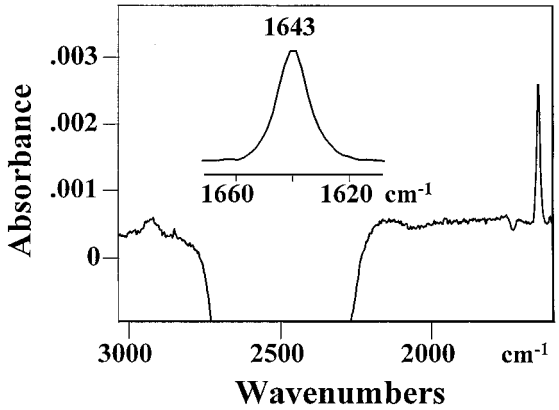

Figure 1. Absorbance is plotted against wavenumber in the infrared spectrum for quaternized polyvinylpyridine (QPVP) adsorbed onto oxidized silicon at pD = 9.2. The large negative band in the region 2750−2250 cm^{-1} shows displacement of D_2O solvent from the surface in order to accommodate positive adsorbed amount of the QPVP polymer. Absorbance of the quaternized pyridinium ring of QPVP, centered at 1643 cm^{-1}, is magnified in the inset. Analysis shows that the integrated absorbance of the QPVP band in this figure corresponds to an adsorbed amount of 1.5 mg m^{-2}.

ATR Spectra. To reduce overlap of the infrared spectra of QPVP with those of water itself, we usually (apart from control experiments which verified that this substitution did not alter the experimental results) dissolved the polymer in D_2O rather than in H_2O.

Figure 1 shows ATR spectra recorded in D_2O. Absorbance is plotted against wavenumber in the infrared region. Most prominent was the intense negative absorption from D_2O; the heavy water was displaced from the near-surface region as QPVP adsorbed, with large infrared intensity because D_2O absorbs infrared radiation strongly in this region. This negative peak from D_2O did not overlap with absorption from functional groups on QPVP, however. In Figure 1, one notices that the intensity of the carbon−hydrogen vibrations (along the chain backbone and in the pyridine ring), located in the neighborhood of 3000 cm^{-1} was so low that they were difficult to resolve. We do not consider them further because the skeletal in-plane vibrations of the pyridinium ring provided similar information with a higher ratio of signal-to-noise. Vibrations of the pyridinium ring, shown magnified in the inset, were centered at 1643 cm^{-1}.

The Amount Adsorbed. Recently we showed[19] that adsorption of QPVP onto oxidized silicon is induced almost entirely by electrostatic attraction to the surface of opposite charge and that the quantity of electrostatically adsorbed polymer increases with increasing hydroxyl content.

In this discussion we refer pD rather than pH, since measurements were performed in D_2O. The amount adsorbed increases with increasing pD until saturation is achieved at high pD.[19] All of the measurements presented in this paper were performed at pD = 9.2—a condition of high surface charge density where the amount of QPVP adsorbed showed minimal dependence on the pD.

The reported $pK_a \approx 9.1-9.4$ of the isolated SiOH group[32] (note that this number appears to be decreased by proximity of other SiOH groups at a solid surface[33]) implies

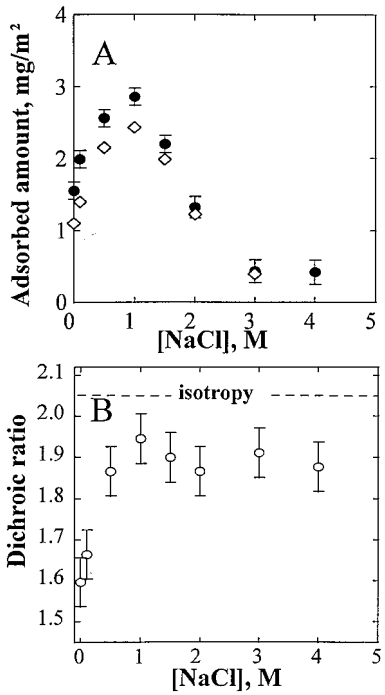

Figure 2. Dependence of the equilibrated adsorbed amount of QPVP (panel A) and the equilibrated dichroic ratio of the 1643 cm^{-1} vibration of the pyridinium ring (panel B). Both are plotted against molar NaCl concentration at pD = 9.2. Circles and diamonds denote adsorption of QPVP onto silicon oxide from concentrations of 1.0 and 0.005 mg mL^{-1} in D_2O, respectively. In panel B, the dotted line indicates the dichroism that corresponds to isotropy.

that, at pD = 9.2, ≈50% of the silanol surface groups on the bare surface were dissociated when the salt concentration was low. This value was further increased by the adsorption of QPVP,[19] yielding ≈80% of dissociated silanol groups at pD = 9.2 and low salt concentration.

To vary the salt concentration systematically, NaCl was added. The pD = 9.2 was regulated with a buffer solution of 1 mM $Na_2B_4O_7 \cdot 10H_2O$. Figure 2A shows the amount of QPVP adsorbed from buffer solutions containing different concentrations of NaCl. As the salt concentration was increased from a low value, the amount adsorbed at first, increasing to double the initial amount. A maximum in the mass adsorbed occurred at 1 M NaCl.

In Figure 2A, the shape of the data were nearly indistinguishable in the cases of adsorption from 0.005 to 1.0 mg mL^{-1} concentration of polymer in solution. However the amount adsorbed from buffer without added NaCl was ≈30% lower in the former case; this, we will see later from Figure 3, was consistent with surface forces experiments.

It is remarkable to see maximum absorbance at the extremely high ionic strength of 1 M—a concentration far too high to be described realistically by double layer considerations. One contribution is certainly that increased screening resulting from decrease of the Debye length reduced the repulsion between adsorbed segments, thereby allowing increasing adsorption. In addition, it is reasonable[6] to consider specific interactions of the polyelectrolyte segments and Na^+ ions with the surface. The competition of small inorganic ions with a polyelectrolyte chain for access to a surface of limited area has also been considered theoretically.[34]

We interpret the data to indicate that the polyelectrolyte adsorbed from low salt concentrations was relatively flat but that increasing salt concentration saw diminished

(32) Perrin, D. D. *Ionization Constants of Inorganic Acids and Bases in Aqueous Solution*; Pergamon Press: New York, 1982; p 99.
(33) Kokufuta, E.; Fujii, S.; Hirai, Y.; Nakamura, I. *Polymer* **1982**, *23*, 452.
(34) Fleer, G. J.; Cohen Stuart, M. A.; Scheutjens, J. M. H. M.; Cosgrove, T.; Vincent, B. *Polymers at Interfaces*; Chapman & Hall: London, 1993.

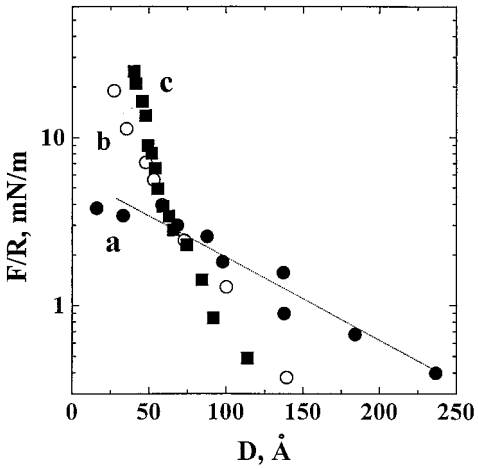

Figure 3. Surface forces (F/R) are plotted against mica−mica surface separation (D) for QPVP adsorbed onto muscovite mica at pH = 9.2. Here F/R indicates the force (F) needed to bring two opposed mica cylinders to the given point of closest separation (D), normalized by the mean radius of curvature of the mica cylinders (R). The data refer to adsorption from concentration 0.005 mg mL^{-1} in H_2O without added salt (curve a), to adsorption from concentration 1.0 mg mL^{-1} in H_2O without added salt (curve b), and to adsorption from concentration 1.0 mg mL^{-1} in H_2O in a solution containing 0.25 M NaCl (curve c). For curve a, we found that at the highest compressive force the surfaces jumped into an adhesive contact with thickness 16 Å (the pull-off adhesive force was then F/R = 30−40 mN m^{-1}).

electrostatic repulsion between neighboring units of the same charge, and this was accompanied by more and more competitive adsorption of Na^+ with the polymer's charged segments for access to surface sites on the silicon surface. At high salt concentrations, the polymer adopted a greater abundance of loops and tails, leading to increasingly more extended layers,[4,12,35−38] and in this process the amount adsorbed doubled.

At the highest salt concentrations, one observes in Figure 2A that the Na^+ actually displaced the polyelectrolyte from the surface, such that increasing the salt concentration provoked less adsorption. At the highest concentrations of Na^+ studied, displacement of the polyelectrolyte was virtually complete. A similar observation, made by Cohen Stuart and co-workers on a different polyelectrolyte system,[39] confirms the generality of this effect. The observed strong dependence of the adsorbed mass on ionic strength was also predicted theoretically.[5,6]

Parenthetically, we note that ionization of surface silanol groups also rises with increased concentration of dissolved salt. This also contributed to the measured increase in the adsorbed amount, but the effect is secondary in importance: it can explain only 20% rise of the amount adsorbed[19] in contrast to the doubling observed. Also, using fully ionized mica at this pH (see below), we corroborated these conclusions by direct force measurements of layer thickness.

Dichroism of Adsorbed Pyridinium Rings. Each repeat unit of QPVP contains a pendant pyridinium ring whose mean orientation relative to the surface was quantified by measuring the dichroic ratio (D), defined in the Experimental Section. While D in this experiment was probably slightly influenced by residual roughness of the polished Si crystals, which gives some uncertainty to the significance of the absolute value, it is meaningful to compare relative values of D measured using the same crystal under different solution conditions. We analyzed D of the carbon−nitrogen stretch at 1643 cm^{-1}, an in-plane stretch. This band is believed to be directed along the symmetry axis of the ring and should reflect the segmental tilt.

Figure 2B shows the dependence of the dichroic ratio on the salt concentration (NaCl). All of the data fell below the dotted line, sketched to indicate the point of isotropy. In "low salt" conditions (adsorption from the buffer alone), the pyridinium rings were most anisotropic, i.e., most preferentially parallel to the surface, but the dichroic ratio increased monotonically with increasing salt concentration until reaching a plateau at which the mean segmental orientation was close to but not quite isotropic.

This observed average near-isotropy is consistent with the looser, fluffier structure that was deduced from the discussion of Figure 2A. In fact, combining the information from parts A and B of Figure 2, it is reasonable to think that pyridinium rings in physical contact with the surface remained relatively flattened while pyridinium rings that dangled into solution were isotropic or nearly so. The average would then be slightly less than isotropic, as observed. It is notable that the maximum mass adsorbed and the plateau dichroic ratio were attained at the same high salt concentration. In addition, as we also noted recently,[19] the surface orientation of pendant rings is also influenced by the polymer's stereoregularity. This polymer was 70% stereoregular, such that it was possible for many adjacent rings along the chain backbone to orient similarly, but for an atactic polymer this would not be possible. Indeed, deviations from isotropy were not observed for the pyridinium rings of an atactic QPVP polymer sample. The influence of a polymer's stereoirregularity precludes quantitative analysis of the dichroism data presented here. The effect is qualitative for a polymer, though for the monomer analogue quantitative interpretation is possible.[28,40]

In arguments presented below, we will use correlations between the average surface orientation of the pyridinium rings in the QPVP molecule and the concentration of salt to distinguish between different nonequilibrium states of the adsorbed QPVP. We will conclude that dichroism of the pyridinium ring depended strongly on the history of adsorption.

I.B. Static Force−Distance Profiles. Next we employed the surface forces technique to obtain independent information about the layer thickness and (in ensuing sections of this paper) its viscoelasticity. The muscovite mica surfaces used in this experiment are known to be completely ionized at pH > 7[41,42] and to carry a high surface charge at our experimental pD = 9.2. Therefore, just as for the FTIR-ATR experiments, the polyelectrolyte adsorption was electrostatically driven.

Figure 3 shows the force−distance profile measured between mica surfaces exposed to dilute solutions of QPVP containing salt of two different concentrations. The scales are semilogarithmic. Force (F) was normalized by the mean radius of surface curvature (R) as is conventional in such measurements. For the case of a low concentration of polymer (0.005 mg mL^{-1}) and no salt except as needed to

(35) Café, M. C.; Robb, I. D. *J. Colloid Interface Sci.* **1982**, *86*, 411.
(36) Cohen Stuart, M. A.; Fleer, G. J.; Lyklema, J.; Norde, W.; Scheutjens, J. M. H. M. *Adv. Colloid Interface Sci.* **1991**, *34*, 477.
(37) van der Schee, H. A.; Lyklema, J. *J. Phys. Chem.* **1984**, *88*, 6661.
(38) Bonekamp, B. C.; van der Schee, H. A.; Lyklema, J. *Croat. Chem. Acta* **1983**, *56*, 695.
(39) Hoogeveen, N. G.; Cohen Stuart, M. A.; Fleer, G. J. *J. Colloid Interface Sci.* **1996**, *182*, 133 and references within.
(40) Sukhishvili, S. A.; Granick, S. *Phys. Rev. Lett.* **1998**, *80*, 3646.
(41) Scales, P. J.; Grieser, F.; Healy, T. W. *Langmuir* **1990**, *6*, 582.
(42) Shubin, V. E.; Kékicheff, P. *J. Colloid Interface Sci.* **1993**, *155*, 108.

produce the buffer solution (10^{-3} M sodium borate buffer, curve a), the forces decayed exponentially. The observed characteristic decay length of 60 Å was close to the 56 Å expected from the DLVO theory for this 1 mM concentration of 1:2 electrolyte. The presence of polyelectrolyte amounted to only 2.3×10^{-5} M of pyridinium units; it contributed in only a minor way to the total ionic strength. It is remarkable that the data followed the same exponential distance dependence down to surface separations as small as 10−30 Å.

Similar observations by other authors on different polyelectrolyte systems[17,43,44] have been interpreted to imply that the adsorbed chains were nestled very flat against the surface. In our experiments (curve a), at the highest compressive force we found that the surfaces jumped into an adhesive contact with thickness 16 Å (the pull-off adhesive force was then $F/R = 30-40$ mN m^{-1}). The amount of QPVP adsorbed was estimated from this final thickness to be 0.8 mg m^2 if one supposes the density of dry QPVP, thus giving an upper bound of the adsorbed amount. We estimate that retention of water within the compressed layer would result in overestimating the adsorbed amount by up to 20%.

For a similar system, a jump of opposed polyelectrolyte layers into adhesive contact from small surface separation was recently interpreted as the effect of van der Waals attraction[44] though bridging of polyelectrolytes between surfaces was proposed earlier by Claesson et al.[45] In the discussion below, based on ancillary information obtained from shear force measurements at large deformation, we will argue that the attraction is rooted principally in bridging interactions between the opposed surfaces. On the theoretical side, the entropically driven bridging between surfaces by polyelectrolyte chains was also identified to be the main cause of attractive forces, especially when the ionic strength is low.[46]

Also shown in Figure 3 is the force−distance profile obtained at still lesser salt concentration but much high concentration of QPVP, 1 mg mL^{-1} (curve b). The amount of QPVP adsorbed under these conditions increased to 1.3 mg m^{-2}, as inferred from measurements of thickness of the adsorbed layers after strong compression. This larger amount adsorbed was accompanied by notable differences in the interaction forces: weakened repulsion at large separations and strong repulsion at separations less than 100 Å. An attempt to approximate the interaction between surfaces at the larger distances by the DLVO repulsion gave 30 Å for the apparent Debye length—a value slightly larger than the expected 24 Å. In the latter value, along with background concentration of the salt in the buffer (10^{-3} M), additional contributions from $\approx 4.6 \times 10^{-3}$ M ions introduced by high concentration of polyelectrolyte (assuming complete dissociation of counterions from the polymer) were taken into account. At smaller distances, the repulsion is enhanced. We interpret this to reflect the entropic forces acting between overlapping tails and loops of the adsorbed polymer. The onset of these forces serves to indicate the extension of the adsorbed layers. Similar appearance of steric repulsion as the concentration of the charged polymer was increased was also found recently by Claesson and co-workers.[47] Note also the disappearance of the short-range attractive force which had been observed when the polyelectrolyte solution concentration (and hence the quantity adsorbed) was lower—the interaction forces for this higher QPVP concentration were repulsive over the whole investigated range of surface separations. Suppression of the bridging attraction between surfaces with increased amount of polyelectrolyte adsorbed is consistent with earlier findings.[45]

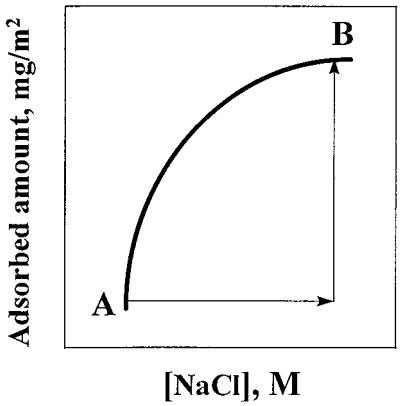

Figure 4. Schematic illustration of the scheme to explore history dependence of adsorption. Polymers were allowed to adsorb either in one step from a given ionic strength of 0.25 or 0.5 M NaCl, or from low salt conditions (buffer being the only source of ions) with 0.25 M NaCl added afterward.

When the concentration of salt in the QPVP solution was increased to a very high value, 0.25 M NaCl, the amount adsorbed as gauged from the thickness at highest compression grew to 1.8 mg m^{-2}, but the force−distance curve at larger distances was almost indistinguishable from curve b. Since curve b was obtained under conditions where the Debye length was 24 Å, but the Debye length was only 6 Å in curve c, it would not be consistent to use a DLVO explanation. The long range was apparently nonelectrostatic, probably reflecting the entropic forces between the adsorbed layers. This suggests that QPVP chains adsorbed on the surface in fluffier conformation, with larger loops and tails. This agrees with other experiments on the polyelectrolyte adsorption.[12,35−38,48,49]

Taken together, these surface forces measurements lead to the same conclusion as the FTIR-ATR experiments: increased ionic strength was accompanied by more adsorption and a larger layer thickness.

II. History Dependence of Adsorption. In this section we investigate differences when QPVP layers were formed from different initial conditions of ionic strength but brought to the final ionic strength. The experimental strategy is sketched in Figure 4.

II.A. Infrared Measurements. Figure 5A shows in situ ATR-FTIR measurements of the amount of QPVP adsorbed when this polymer was first allowed to adsorb from low salt concentration (buffer alone), and then after equilibration the polymer solution was successively replaced by buffer solutions of increasingly higher salt concentration (0.1 M and 0.5 M NaCl). Since no QPVP was present in the solution, no subsequent adsorption occurred. The data also show that no desorption ensued, probably because of the prohibitively high activation energy required for desorption.

In contrast to the minimal dependence of the adsorbed amount on adsorption history (Figure 5A), Figure 5B shows that the dichroic ratio of the pyridinium rings

(43) Claesson, P. M.; Dahlgren, M. A. G.; Eriksson, L. *Colloids Surf., A* **1994**, *93*, 293.
(44) Hartley, P. G.; Scales, P. J. *Langmuir* **1998**, *14*, 6948.
(45) Dahlgren, M. A. G.; Waltermo, Å.; Blomberg, E.; Claesson, P. M.; Sjöström, L.; Åkesson, T.; Jönsson, B. *J. Phys. Chem.* **1993**, *97*, 11769.
(46) Miklavic, S. J.; Woodward, C. E.; Jönsson, B.; Åkesson, T. *Macromolecules* **1990**, *23*, 4149.
(47) Dahlgren, M. A. G.; Claesson, P. M.; Audebert, R. *J. Colloid Interface Sci.* **1994**, *166*, 343.
(48) Marra, J.; Hair, M. L. *J. Phys. Chem.* **1988**, *92*, 6044.
(49) Kamiyama, Y.; Israelachvili, J. *Macromolecules* **1992**, *25*, 5081.

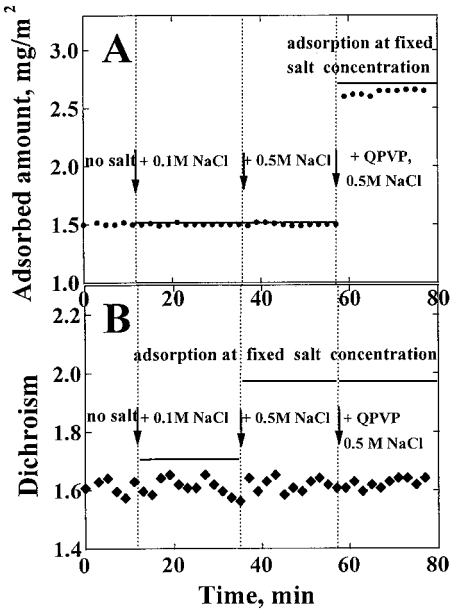

Figure 5. This figure contrasts the influence of adding salt before or after adsorption. The data refer to the adsorption of QPVP onto silicon oxide (from 1.0 mg mL^{-1} in D_2O buffered at pD = 9.2). In one sequence, indicated by data points, the polyelectrolyte was first allowed to adsorb from buffer solution with no added salt, then later this solution was replaced by the same buffer containing 0.1 M NaCl, then later by the same buffer containing 0.5 M NaCl, and finally replaced by a solution of QPVP (same concentration as for the initial adsorption) in 0.5 M NaCl. In the alternative adsorption history, indicated by solid horizontal lines, the same QPVP polymer was allowed to adsorb in one step from the given NaCl concentration. One observes that adsorption history caused minor differences in adsorbed amount (panel A) but large differences in dichroism of the 1643 cm^{-1} vibration of the pyridinium ring (panel B).

pendant to this polymer showed strong dependence on the history of adsorption. When the salt concentration was raised stepwise from low to higher levels, the dichroic ratio remained fixed at the level it took upon initial adsorption, persistently showing the same relatively high degree of anisotropy. The contrasting case of adsorption directly from the given salt concentration resulted in near isotropy, however. In Figure 5B, these latter values are indicated as horizontal bars; these data are taken from raw data in Figure 2B. The contrast between parts A and B of Figure 5 shows that the amount adsorbed should not be used as the sole criterion whether an adsorbed layer equilibrates.

It will be desirable, in future work, to perform similar measurements using a polymer in which the chain backbone itself could be resolved by measurements of the infrared dichroism. This, unfortunately, was not possible to resolve for QPVP. Measurements employing adsorbed poly(ethylene imine) are underway.

II.B. Surface Forces Measurements. Adsorption of the polymer was first allowed to occur from the buffer solution with no salt added, then the ionic strength of the solution was increased by adding an equal volume of the buffer containing high salt concentration (0.5 M NaCl). The concentration of salt in the final polymer solution was therefore 0.25 M NaCl. The force−distance profile measured in this case of two-step adsorption is plotted in Figure 6. Also shown here is the force−distance profile for adsorbed QPVP layers produced by one-step adsorption at the same final salt concentrations. Both force−distance profiles are monotonically repulsive, but the one produced from two-step adsorption is roughly twice as thick at the

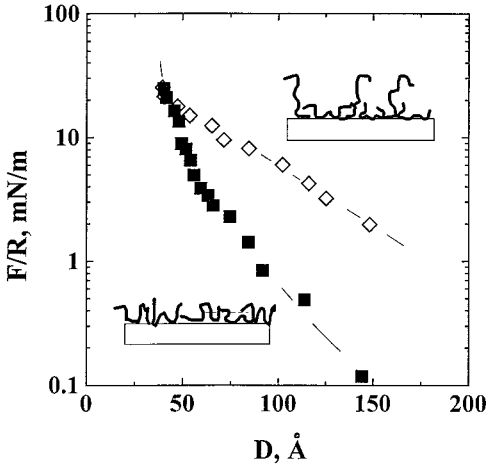

Figure 6. This figure contrasts the influence on surface forces of adding salt before or after adsorption. Surface forces (F/R) are plotted against mica−mica surface separation (D) for QPVP adsorbed onto muscovite mica at pH = 9.2. Here F/R indicates the force (F) needed to bring two opposed mica cylinders to the given point of closest separation (D), normalized by the mean radius of curvature of the mica cylinders (R). The two data sets refer to QPVP (1 mg mL^{-1} in H_2O at pH = 9.2) allowed to adsorb from buffer solution first with no added salt but 0.5 M NaCl added later to produce the final concentration 0.25 M NaCl (open diamonds) or from a solution containing 0.25 M NaCl (filled squares). One observes that while the adsorbed amount in the two cases is similar, the range of surface forces is very different. The inset shows a hypothetical sketch of the different polyelectrolyte configurations resulting from two-step or one-step adsorption to the same final solution state.

point of onset of significant forces.

We know from Figure 5A that the adsorbed amount was similar in two such cases, and the generality of that conclusion is strongly suggested by the observation, in Figure 6, that the films could be compressed to the same ultimate layer thickness regardless of adsorption history. Both sets of data show a hard wall of steep repulsion at 36 Å, corresponding to adsorbed amounts of ≈1.8 mg m^{-2}. These estimates of adsorbed amount agree qualitatively with the direct infrared-based measurements presented in Figure 2 for adsorption onto a different surface (oxidized silicon) but under similar conditions of large surface charge.

A reasonable scenario to explain the large difference in layer thickness, despite the similar amount adsorbed, is the following. When chains adsorb in the one-step process from a low ionic strength, it is known that they adsorb relatively flattened. Further adsorption takes place when the salt concentration is raised, but with the constraint, because of the segment-surface interaction enthalpy is so strong for electrostatically driven adsorption, that the flattened configurations of the initial structure will be retained for a long time. The result will be that later-arriving chains will adsorb at a relatively small number of potential adsorption sites and will therefore extend far into solution. Conversely, when chains adsorb in the one-step process from a higher ionic strength, chain configurations within the resulting layer will be more nearly homogeneous.

A similar picture had emerged previously for nonpolar polymers adsorbed from a nonpolar solvent; it was proposed, based on dichroism measurements, that chains which adsorb onto a previously adsorbed layer possess a more extended conformation than at equilibrium.[50,51] Recently we suggested the same concerning adsorbed polyelectrolytes.[11] Figure 6 offers additional evidence to support this picture.

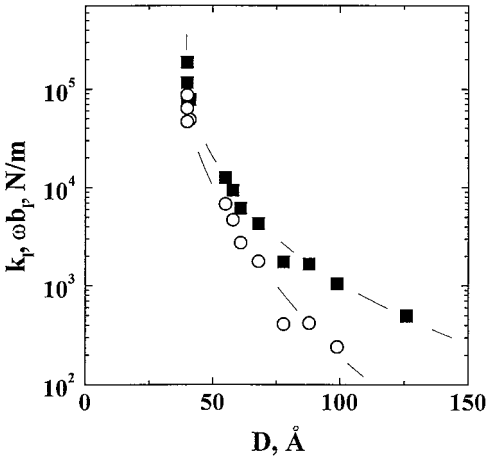

Figure 7. Shear constants are plotted against mica−mica closest surface separation (D) for QPVP adsorbed from a concentration of 1 mg mL^{-1} in H_2O onto muscovite mica at pH = 9.2 and 0.25 M NaCl. In response to oscillatory forces applied at 256 Hz, from the resulting displacement the resistance to shear was decomposed into one component in phase with the drive, the elastic response (k_L, squares) and a second component 90° out of phase with the drive, the viscous response (ωb_L, circles). These shear constants are defined as shear force normalized by shear displacement under conditions of small displacement ("linear response") where force was proportional to displacement.

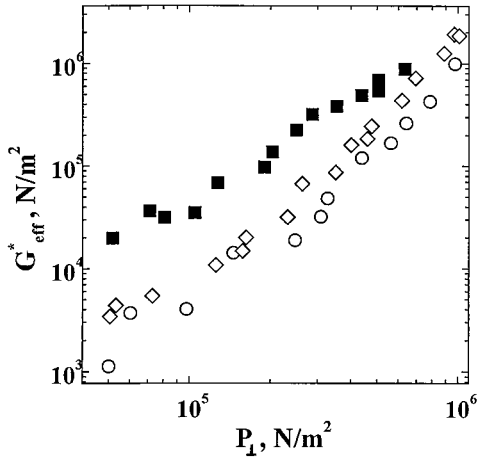

Figure 8. Coupling of force constants in the shear direction (measured in linear response regime at 256 Hz) to static force in the orthogonal normal direction. The data show the difference between adding salt before or after adsorption. Shear force constant refers here to the root-mean-square of the elastic and viscous force constants measured at 256 Hz. In addition, forces were normalized by the effective contact area and film thickness (see text) in order to express shear force constants as an effective shear modulus, G_{eff}*, and normal forces as pressure directed in the normal direction, $P_\perp$. The three sets of data refer to QPVP adsorbed from a concentration of 1 mg mL^{-1} in H_2O onto muscovite mica at pH = 9.2 in the presence of no added salt (open circles), in the presence of 0.25 M NaCl (squares), or with no added salt during the adsorption step but 0.5 M NaCl added after equilibration of the amount adsorbed to produce the final concentration 0.25 M NaCl (open diamonds).

In other words, the data suggest that one-step adsorption produces a relatively homogeneous layer, whereas two-step adsorption produces a layer divided into two regions: relatively dense segmental density (closest to the surface) and relatively sparse farther away. A hypothetical sketch of the respective chain configurations in these two types of adsorbed layers, produced by these two patterns of adsorption history, is sketched in the inset of Figure 6.

II.C. Shear Nanorheology. If the interpretation just presented is valid, differences between one-step and two-step adsorption should also manifest themselves in dynamical properties of the adsorbed layers. For one-step adsorption (formed in one step from 0.25 M NaCl solution), the elastic and viscous force constants at 256 Hz are plotted against film thickness in Figure 7. These experiments were performed with small deformations, <10 Å shear amplitude, small enough to produce a linear response. The onset of measurable shear forces was at approximately the same film thickness as the onset of measurable forces in the normal direction, indicating that both phenomena stemmed in similar measure from the overlap of opposed layers. In control experiments, this same trend was observed under conditions of other ionic strength: shear dynamic forces first became enhanced over the bulk response at a similar surface separation as for the static forces.

However, it is curious to see that the elastic component of shear force always exceeded the viscous component. This contrasts with our experience with numerous systems in nonpolar media that we have studied in the past, concerning both polymers[52] and small molecules,[53] where the response was always predominantly viscous provided that the film thickness was sufficiently large. The reason for enhanced shear elasticity in the present polyelectrolyte system is not yet understood (we note that a possible explanation was proposed recently[54]). However, both the elastic and viscous forces increased rapidly as the layers were more compressed.

To explore more quantitatively the coupling between shear forces and forces in the normal direction, at first we calculated their ratio, the friction coefficient. For this purpose we took the root-mean-square of the elastic and viscous force constants, to express shear force constant as a single number, and normalized by the effective contact area, A_{eff} and film thickness, D, to give an effect shear modulus, G_{eff}*. (Here $A_{eff} \approx 2\pi RD$ in the Langbein approximation,[55] where R is mean radius of curvature of the mica surfaces and D is their separation.) Specifically

$$G^*(\omega) = [(f_{elastic}(\omega)/d)^2 + (f_{viscous}(\omega)/d)^2]^{1/2}[D/A_{eff}] \quad (3)$$

where the symbol, d, refers to the shear amplitude in oscillatory deformation. The elastic force constant is $f_{elastic}(\omega)/d$ and the viscous force constant is $f_{viscous}(\omega)/d$.

The normal pressure was defined similarly as

$$P_\perp \approx F_\perp/2\pi RD \quad (4)$$

where $F_\perp$ is the static surface force needed to squeeze the polymer layer to a given film thickness, D.

In Figure 8, G_{eff}* is plotted against $P_\perp$; this representation allows one to compare the shear moduli at constant levels of normal pressure. One observes that the shear modulus at small normal pressure was larger by about an order of magnitude for one-step adsorption. The difference diminished somewhat with increasing normal pressure but persisted even for the largest normal pressures that

(50) de Gennes, P.-G. In *New Trends in Physics and Physical Chemistry of Polymers*; Lee, L.-H., Ed.; Plenum: New York, 1990.
(51) Cohen Stuart, M. A.; Fleer, G. J. *Annu. Rev. Mater. Sci.* **1996**, *26*, 463.
(52) Hu, H.-W.; Granick, S. *Science* **1992**, *258*, 1339.
(53) Demirel, A. L.; Granick, S. *Phys. Rev. Lett.* **1996**, *77*, 2261.
(54) Safran, S. A. *Phys. Rev. Lett.* **1998**, *81*, 4768.
(55) Israelachvili, J. N. *Intermolecular and Surface Forces*; Academic Press: London, 1992.

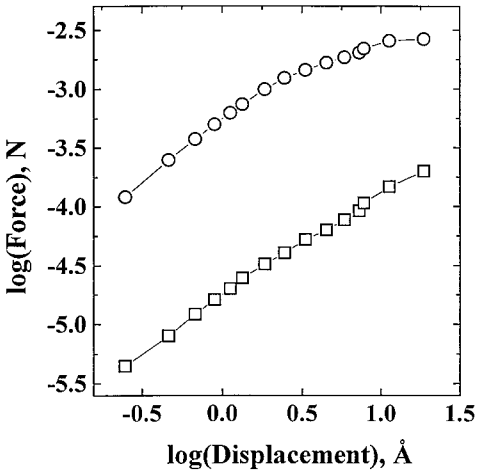

Figure 9. Shear forces are plotted against displacement. Circles denote elastic forces (in phase with the oscillatory displacement at 256 Hz) and squares denote dissipative forces (90° out of phase). The data concern QPVP adsorbed from a concentration of 0.005 mg mL^{-1} in H_2O onto muscovite mica at pH = 9.2 in borate buffer with no added salt. The transition to nonlinear shear forces occurs at ≈30−60 pN $chain^{-1}$, as also does the adhesion, as discussed in the text.

were applied. In addition, it is fascinating to observe that at a given normal pressure, the shear modulus for two-step adsorption (high salt) was indistinguishable from that obtained for one-step adsorption from low salt concentration.

The differences in the dynamic response of the adsorbed QPVP and history are evident in the results shown in Figure 8. For the case of a dense layer, the dynamic forces increase rapidly with the onset of static pressure. However, in the case where the structure is more extended, one observes weaker dynamic forces compared to dense adsorbed layers at higher salt concentrations. An extreme analogy would be that with a brushlike layer where the shear resistance is very low even at high static forces. When the layers are more compressed, the effects of salt concentration are more governed by the adsorbed amount, as expected.

This decoupling of shear from normal forces, in the case of two-step adsorption, is perhaps analogous to the results of Klein and co-workers for the shear of nonpolar polymer brushes in a good solvent.[56] These workers elegantly demonstrated that though end-attached polymer chains in solvent ("polymer brushes") strongly resist being pressed together for thermodynamic reasons, their interfacial sliding over one another may be dominated by an entirely different physical mechanism. The hypothetical conformations discussed above and sketched in the inset of Figure 6 would also be expected to result in brushlike conformations within the outermost "spare" portions of the adsorbed layers formed in a two-stage adsorption process. Denser layers formed from the one-step adsorption process displayed, at a given normal pressure, much higher shear modulus. However when the two-step layers were highly compressed, their resistance to shear was governed more by adsorbed amount than by history of adsorption, as expected. To decouple shear and normal forces comprises another approach to minimize "friction", by allowing friction forces to remain small even as normal forces become large.

It was an interesting sidelight to also explore how these systems responded to deformations of amplitude so large that instabilities would result. We present here (Figure 9) results for only one system, polymer allowed to adsorb from very low concentration in the absence of added salt such that a very thin adsorbed layer resulted, to show the character of the results. In Figure 9, elastic and viscous shear forces are plotted against deformation amplitude. One sees at first the regime of linear response (the concern of earlier figures in this paper), followed by nonlinear response. It is intriguing that the elastic shear force at the onset of nonlinearity (1×10^{-3} N) is reasonably close to the adhesive force required to separate these surfaces ($(5-6) \times 10^{-4}$ N). This suggests that a similar mechanism, the detachment of bridged chains from an adjoining surface, lay at the root of both the shear and the adhesion instability.

The adsorbed amount, ≈0.8 mg m^{-2}, is equivalent (using the flattened contact area) to $\approx 3.5 \times 10^7$ chains within the contact area. The shear yield force and the adhesive force then amount to ≈30−60 pN $chain^{-1}$ under the assumption that every chain contributed to these forces. Direct atomic force microscopy studies of molecule−molecule adhesion[57] or polymer−surface adhesion[58] give numbers of the same magnitude.

Conclusions and Outlook

We have studied in this paper, using a combination of experimental methods, the path dependence of various features of a model adsorbed charged polymer at the relatively high salt concentration of 0.25 M NaCl. The adsorbed amount showed little dependence on path, thus validating the common assumption of equilibration in this respect. However several other properties—surface forces, shear nanorheology, and orientation of pendant side groups of the polymer—all showed a pronounced dependence on the path to reach the adsorbed state.

One practical conclusion is that two-step adsorption (adsorption at low salt concentration, followed by adding salt) produced thicker layers than one-step adsorption to produce the same final salt concentration. The result was to tend to decouple shear forces from those that resist compression in the normal direction, thereby lessening the shear forces at a given level of normal force. We have hypothesized that the underlying chain conformations may be comprised of a dense layer of chains closest to the solid surface and a sparse outer layer.

A second practical conclusion is to qualify the view, sometimes found in current literature, that charged polymers behave as if they were uncharged when the salt concentration is raised to a level sufficient to screen the electrical charges. This study suggests that a more complex situation holds in the common case where the polymer resides at a solid surface because of electrostatic attraction to it. In this case the polymer surface configuration retains a long memory of the history of adsorption, owing to the large adsorption energy. The existence of history-dependent configurations makes adsorbed layers susceptible to deliberate, rational manipulation of not only a layer's thickness but also the friction when opposed layers slide over one another.

Acknowledgment. This material is based upon work supported by National Science Foundation and by the U.S. Department of Energy through the Frederick Seitz Materials Research Laboratory at the University of Illinois at Urbana-Champaign.

LA990679O

(56) Klein, J.; Kumacheva, E.; Mahalu, D.; Perahia, D.; Fetters, L. J. *Nature* **1994**, *370*, 634.
(57) Florin, E. L.; Moy, V. T.; Gaub, H. E. *Science* **1994**, *264*, 415.
(58) Ortiz, C.; Hadziioannou, G. *Macromolecules* **1999**, *32*, 780.